Published in final edited form as:
Neurosci Lett. 2011 January 20; 488(2): 123–128. doi:10.1016/j.neulet.2010.11.013.

Dynamic task-specific brain network connectivity in children with severe reading difficulties

Michael Vourkas[1], **Sifis Micheloyannis**[2], **Panagiotis G. Simos**[3], **Roozbeh Rezaie**[4], **Jack M. Fletcher**[5], **Paul T. Cirino**[5], and **Andrew C. Papanicolaou**[4]

[1]Technological Education Institute of Crete, Heraklion Crete, 71004 Greece

[2]Research Clinical Neurophysiological Laboratory Widén, Medical Division, University of Crete, Heraklion, Crete, 71409 Greece

[2]Department of Psychology, University of Crete, Rethymno, Crete, 74100 Greece

[4]Department of Pediatrics, Children's Learning Institute, University of Texas Health Science Center at Houston, Houston, Texas, 77030 USA

[5]Department of Psychology, University of Houston, Houston, Texas, 77204 USA

Abstract

We investigated patterns of sensor-level functional connectivity derived from single-trial whole-head magnetoencephalography data during a pseudoword reading and a letter-sound naming task in children with reading difficulties (RD) and children with no reading impairments (NI). The Phase Lag Index (PLI), a linear and nonlinear estimator, computed for each pair of sensors, was used to construct graphs and obtain estimates of local and global network efficiency according to graph theory. In the 8 to 13 Hz (alpha band) and 20–30 Hz (gamma band) range, RD students showed significantly lower global efficiency than NI children, for the entire MEG recording epoch. RD students also displayed reduced local network efficiency in the alpha band. Correlations between phonological decoding ability and graph metrics were particularly evident during the task that posed significant demands for phonological decoding, and followed distinct time courses depending on signal frequency. Results are consistent with the notion of task-dependent, aberrant long- and short-range functional connectivity in RD children.

Keywords

Phonological decoding; dyslexia; magnetoencephalography; connectivity, graph theory; small-world networks

Numerous functional imaging studies have shown that children with word level reading difficulties (RD) exhibit reduced neurophysiological and hemodynamic activity in several posterior temporal, inferior parietal, occipito-temporal, and inferior frontal regions, mainly in the left hemisphere [e.g. 4,17,20,21]. Correlations between behavioral and hemodynamic data imply that RD is associated with an impairment of the brain network underlying

Correspondence concerning this article should be addressed to: Michael Vourkas Technological Education Institute of Crete, Estavromenos/Iraklion Crete, 71004 Greece. Tel +302810379806, +306946506781, vourkas@teicrete.gr.

reading, which may result from inefficient or inadequate neuronal connections between key cortical regions comprising this circuit, including the angular gyrus [2,6,8,11,16]. This notion is further supported by magnetoencephalography (MEG) studies, which have demonstrated differences in the relative timing of the engagement of brain structures critical to the reading mechanism between RD and NI groups [19,20,21].

Recent methodological developments in network analysis of bioelectrical signals have emerged as promising tools for the evaluation of real-time neural connectivity, primarily at the sensor level. Two well-known parameters derived from graph theory are local and global efficiency, with the former providing a measure of local effective connectedness, and the latter a measure of overall effective integration. These two measures form the basis for computing an index of "small-world" network (SWN) organization [20]. An SWN is an ideal network model characterized by high global and local efficiency indices [7,13,24].

In the present study, we applied measures of local and global efficiency as well as the concept of SWN to investigate patterns of functional connectivity, at the sensor level, derived from single-trial whole-head MEG data during performance of two reading tasks. We sought to address whether phonological decoding, assessed using tasks varying in the degree of relative difficulty, are associated with different patterns of surface-level network organization in groups of students with RD and typical development of reading skills and comparable in age, gender, and of at least average intelligence.

The target sample included 12 children (8 boys, mean age 123 ± 23 months) with reading difficulties (RD group) as indicated by scores below the 16thpercentile (standard score of 85) on the Basic Reading composite (average of Word Attack and Letter-Word Identification subtest scores of the Woodcock-Johnson Tests of Achievement-III [28] (range 64–84; W-J III). A second group of 15 children (13 boys, mean age 117 ± 29 months) who had never experienced difficulties in reading (NI group) served as comparisons, having standard scores > 95 on the Reading Composite index (corresponding to the 36thpercentile). All participants had Full Scale IQ scores > 80 on the Wechsler Abbreviated Scale of Intelligence [27]. Table 1 displays demographic and psychoeducational information for each of the two groups of participants, which were not significantly different on age, gender, ethnicity, handedness, Verbal, and Performance IQ. Exclusion criteria included history of neurological or psychiatric disorder (including ADHD).

Tasks. Each participant was tested on two naming tasks that varied on decoding difficulty. For the *letter-sound task*, stimuli were four randomized sequences of 24 single, lowercase letters subtending 0.6° of visual angle. For the *pseudoword reading task*, stimuli were three-letter pronounceable non-words (e.g., *lan*), subtending 2.0° of visual angle [17].

MEG recordings were obtained with a whole-head neuromagnetometer array (4-D Neuroimaging, Magnes WH3600), consisting of 248 first-order axial gradiometer coils, housed in a magnetically shielded chamber. For each task 84–143 artifact free epochs (filtered between 0.1 and 40 Hz, digitized at 254 Hz and spanning between −140 to 800 ms in relation to stimulus onset) were available for each participant and task. Single-trial epochs were visually inspected excluding those that contained potential artifacts defined as peak-to-peak amplitudes > 2 pT. The two groups did not differ on the number of artifact-free epochs ($p > .1$).

Estimation of channel interdependencies was based on the Phase Lag Index (PLI) [23] computed between all pairs of MEG channels. This index is based on the presence of a systematic phase difference between two time-series which will show up as an asymmetry in the corresponding distribution. PLI values were computed with a resolution of 1Hz in frequency and 30 ms in time domain. Here, we use a modified version of PLI which utilizes

ensemble averaging across trials instead of time averages, in order to achieve time-dependent estimators of phase difference dynamics. The required phases of the MEG signals can be extracted from the complex coefficients of their continuous wavelet transform [12]. If the relative phase distribution is centered around zero, PLI is also zero indicating either no coupling or coupling with phase difference centered around zero. For a perfect phase locking at a non-zero phase difference the PLI is equal to one. PLI values significantly different than zero indicate non-negligible inter-dependence between the sensors in a particular pair. Significant PLI values were determined after calculating PLI for surrogates derived by randomizing the order of trials in one of the channels of each pair [9]. Significance levels were then extracted from the z-scores of the difference between PLI values in the original and surrogate data. Significance probabilities were corrected using the false discovery rate (FDR) method in order to correct for multiple comparisons [3].

Although the phase-lag index is less sensitive to volume conduction and field spread effects than phase coherence, it is not immune to these effects especially when axial gradiometer data are involved [see e.g. 18]. In order to ensure that PLI-related group effects reflected differences in regional connectivity rather than differences in the levels of oscillatory activity or signal-to-noise ratio, we computed estimates of spectral density and noise levels for each sensor and task. The power spectral density (PSD) of each sensor was assessed by averaging the multiple trials PSDs which in turn were estimated by the modified periodogram method using a hamming window. The relative power of each frequency band was then computed as the ratio of the power of the corresponding band and the total power of the signal. In addition, the average field strength during the 140-ms prestimulus period was computed for each epoch as an index of stimulus-irrelevant (background) activity. In order to reduce the number of comparisons in the analyses of the PSD and noise data, summary estimates were computed for groups of sensors within six sectors overlaying frontal, central, parietal, temporal, occipito-temporal, and occipital regions.

Graph properties

Functional connections that survived PLI significance tests served as the undirected edges of binary graphs. The structural properties of the resulting functional graphs were analyzed using three well known parameters in graph theory: mean degree K, global efficiency E_{glob} and local efficiency E_{loc} [10,22,24]. The small-world behaviour of functional networks was explored using a set of random surrogate networks. The values of global and local efficiency were compared to the corresponding values of “equivalent” random graphs generated according to a procedure that preserves the degree distribution [22]. For each subject, thirty random graphs were generated and the average values of E_{glob} and E_{loc} were compared to the ones of the original MEG data according to the normalized efficiencies $\varepsilon_{glob}=E_{glob}/E^{r}_{glob}$ and $\varepsilon_{loc}=E_{loc}/E^{r}_{loc}$. Typically, the global efficiency of a network with Small World characteristics is close to but less than the corresponding efficiency of random networks which leads to $\varepsilon^{sw}_{glob}<1$ (and close to 1). On the other hand, a SWN should exhibit significantly higher local efficiency values compared to random networks, as indicated by normalized efficiency values $\varepsilon^{sw}_{loc} \gg 1.0$. An additional measure of the local groupings of significant nodes was computed as the *modularity* metric using the formula, proposed by Newman [14] for the identification of possible community structure in complex networks. Modularity (Q) quantifies the quality of the overall partitioning of the network defined by the appearance of groups of nodes that are more densely connected internally than with the rest of the network.

The time-frequency resolution of the calculated graph measures (*Eglob, Eloc, K, Q*) was reduced by averaging across four frequency bands (4–7 Hz, 8–13 Hz, 14–19 Hz, and 20–30

Hz), and 13 time bins (1 pre-stimulus: 140 ms, 12 post-stimulus: 60 ms). The average graph parameters were then submitted to ANOVAs with Task (letter-sound/pseudoword) and Time bin (13) as the within subjects variables, and Group (NI/RD) as the between subjects variable. Significant two- or three- way interactions involving Group were further evaluated by performing one- or two- way ANOVAs, respectively (Group, or Group*Time within each task). All ANOVA results were evaluated using the Huynh-Feldt method as a precaution against inhomogeneity of variance problems. In addition, Pearson correlation coefficients were computed between reading measures and graph parameters. PSD data were submitted to ANOVAs with Sensor Sector (frontal, central, parietal, temporal, occipito-temporal, occipital) and hemisphere (left, right) as the within subjects factors and Group as the between subjects factor, separately for each band (theta, alpha, beta, gamma).

Inspection of normalized global efficiency values across participants, frequency bands, and latency windows revealed distributions with a mean slightly lower than 1.0, suggestive of the presence of small-world characteristics in the sensor-level network. For the Letter Sound task mean ε_{glob} values were .902±.059 (NI group) and .885±.074 (RD group). Corresponding values for the Pseudoword reading task were: .892±.064 and .888 ±.076.

With respect to raw *Global Efficiency values*, group effects (NI>RD) were restricted to the alpha (group main effect: $F[1,25] = 14.20$, $p < .001$) and gamma bands (group main effect: $F[1,25] = 6.24$, $p < .02$) (Figure 1). Additionally, significant Task main effects were found in the beta, $F(1,25) = 10.10$, $p < .004$, and gamma bands, $F(1,25) = 14.74$, $p < .001$, indicating greater global efficiency during performance of the less demanding letter-sound, as compared to the pseudoword reading task across groups.

The NI group showed higher *mean Degree (K)* indices compared to the RD group across task and latency windows in the alpha band (Group main effect: $F[1,25] = 8.94$, $p < .006$). Task differences (Letter Sound > Pseudoword) were found in the alpha, $F(1,25) = 5.51$, $p < .02$, gamma bands, $F(1,25) = 13.21$, $p < .001$. A similar pattern was present for *Local Efficiency*, with higher values for the NI as compared to the RD group across tasks and time windows in the alpha band, $F(1,25) = 10.30$, $p < .004$, and higher values for the Letter Sound than the Pseudoword task in the alpha, $F(1,25) = 5.44$, $p < .02$, and gamma bands, $F(1,25) = 11.98$, $p < .002$. Analyses on the Modularity index (Q) revealed significantly higher values for the RD as compared to the NI group. These effects were restricted to the alpha band and reached significance ($p < .005$) between 120 and 660 ms for the letter-sound task and between 300 and 420 ms for the pseudoword task ($p < .01$).

Group differences on PSD measures were restricted to the parietal sensor sectors in the alpha band as indicated by a significant Group by Sector interaction, $F(5,125) = 3.06$, $p < .01$ (simple main effect of group showing NI>RD: $F[1,25] = 5.65$, $p < .03$).

With respect to the overall amplitude of prestimulus magnetic flux, which was used as an estimate of the magnitude of task-irrelevant activity, we only found a tendency for higher amplitudes among NI as compared to RD students during the pseudoword task, across sensor sectors, as indicated by a Group by Task interaction, $F(1,25) = 5.26$, $p < .03$ (simple main effect of group: $F[1,25] = 5.13$, $p < .03$).

Pearson correlation coefficients between graph indices and WJ-Word Attack standard scores were significant ($.60 > r > .50$, $p < .01$) for signals in the theta, alpha, and gamma bands. Time plots of correlation coefficients revealed interesting trends: significant correlations were restricted to the alpha band during performance of the Letter Sound task and they were present during the entire recording epoch. As shown in Figure 2, the mapping between decoding ability and graph metrics was present over a wider range of signal frequencies but with distinct time courses during pseudoword reading: Correlations in the theta band were

restricted to late latencies (660–800 ms), correlations in the alpha band were present at middle and late latencies, whereas ability-graph metric associations in the gamma band were strongest at early latencies (0–330 ms). These correlations were mostly driven by group membership, however, rather than systematic covariation across participants within each group, as shown in the scatter-plot in Figure 3. The fact that participants were selected in order to maximize group differences on reading ability may in part contribute to this trend.

In the present study we found significantly reduced global and local efficiency indices in hypothetical sensor-level networks for children with RD than for typical readers. Group differences were noted across the entire recording epoch and were present for both decoding tasks. However, significant across-group linear associations between graph parameters and decoding ability were noted over a wider range of MEG signal frequencies (theta, alpha, and lower gamma) in response to printed stimuli that posed higher demands for phonological decoding (pseudowords vs. single letters). Moreover, the temporal pattern of significant ability-MEG correlations revealed frequency specificity: efficiency of both global and regional (hypothetical) transfer of information correlated strongly with decoding ability close to stimulus onset in the lower gamma band, and after approximately 660 ms in the theta band. Corresponding correlations persisted throughout the recording epoch in the alpha band. Conversely, latency-independent correlations between decoding ability and graph parameters computed during the letter naming task were restricted to the alpha band.

The findings are consistent with rapidly accumulating evidence for disrupted long-range connectivity as one (or the main) characteristic of the neural basis of RD. Several studies point to specific, rather than diffuse, reductions in the integrity of long-range connections between posterior and anterior brain regions [2,15,25]. These developmental changes may in turn have an impact on the efficiency of neural communication between remote brain regions which may become more apparent when the demands for distant neuronal signaling are increased depending on specific task requirements. Interestingly, a complementary measure of local organization, modularity, revealed the presence of a highly partitioned sensor array among RD participants (at least in the alpha band), characterized by groups of sensors that show dense intrinsic inter-dependencies.

These findings are consistent with recent developments in the mapping of the anatomical connections between key cortical regions for reading [eg. 2,5]. Tasks that require mental conversion of print into sound (active phonological and complex articulatory representations), such as the pseudoword reading task used in the present study, are expected to pose increased demands for neuronal signalling between posterior (occipito-temporal and temporoparietal) and anterior regions (inferior frontal cortices) comprising the brain mechanism for reading. As these long-range connections are less efficient than in children with typical reading development they may not be capable of accommodating heightened neuronal signalling demands, leading to reduced global efficiency values.

Alternative interpretations of these findings may take into account potential group differences in spectral power and/or in background (i.e., task-irrelevant activity). Additional analyses revealed minimal group differences on these parameters: a tendency for greater spectral power for NI participants was restricted to the alpha band at parietal sensors. However, NI students displayed higher noise estimates than the RD group across sensors, although this difference was restricted to the pseudoword reading task. Without entirely precluding potential confounding effects of group differences in the power of rhythmic activity, these findings render this account unlikely for the entire range of effects in local and global sensor interdependencies.

An important note concerns the possibility of spurious inter-relations between magnetic fields that form dipolar contours on sensor space. Although this problem is not likely to affect the internal validity of global efficiency estimates, it precludes conclusions regarding the underlying cortico-cortical connectivity patterns that are implicated in phonological decoding. Alternative accounts of the present findings include reduced degree of regional activity, mainly in temporoparietal areas, which has been documented repeatedly in MEG and hemodynamic studies [e.g. 17,19,20,21]. This possibility is minimal, however, since the present findings are based on "raw" single-trial MEG recordings using a technique which is unlikely to be affected by overall signal amplitude. In contrast, previous MEG studies reporting regional hypoactivation assessed time-locked activity, mainly in lower frequency bands, suitable for source localization and estimation. The specificity of the findings is further attested by the fact that less-than-optimal network organization was restricted to the upper electromagnetic frequency bands.

Graph-theory based algorithms complement traditional linear approaches exploring functional interactions between cortical regions and have already been applied to a variety of behavioral/cognitive activation conditions in typically developing, as well as neurologically and functionally impaired, individuals [e.g. 1,10,24].

Future studies should address specific hypotheses regarding the scalp distribution of network changes as a means to assess the potential spatial specificity of group effects associated with phonological decoding and word recognition (see for instance [7]). By taking advantage of recent developments in anatomical knowledge regarding key cortico-cortical connections involved in the reading mechanism in conjunction with the millisecond-level temporal resolution of MEG recordings future investigations should explore parallel patterns of functional interdependencies between occipito-temporal, temporo-parietal and inferior frontal regions that enable reading. Studies that simultaneously coregister structural and functional imaging modalities may be especially useful in elucidating these structure-function relations.

Research Highlights

- Instantaneous phase of MEG signals is extracted using continuous Morlet wavelet.
- Binary undirected Graphs are formed by the significant Phase Lag Index.
- Graphs are explored using the mean degree, the global-, and local-efficiency.
- Small world network was preserved in Reading Disabled and Normal Readers.
- Reading Disabled and Normal Readers were distinguished by the graph parameters.

Acknowledgments

This research was supported in part by grant P50 HD052117 from the Eunice Kennedy Shriver National Institute of Child Health and Human Development (NICHD). The content is solely the responsibility of the authors and does not necessarily represent the official views of the NICHD or the National Institutes of Health.

References

1. Bassett DS, Bullmore ET. Human brain networks in health and disease. Curr Opin Neurol. 2009; 22:340–347. [PubMed: 19494774]

2. Beaulieu C, Plewes C, Paulson LA, Roy D, Snook L, Concha L, Phillips L. Imaging brain connectivity in children with diverse reading ability. NeuroImage. 2005; 25:1266–1271. [PubMed: 15850744]
3. Benjamini Y, Hochberg Y. Controlling the False Discovery Rate: A Practical and Powerful Approach to Multiple Testing. Journal of the Royal Statistical Society. Series B (Methodological). 1995; 57:289–300.
4. Cao F, Bitan T, Chou T-L, Burman DD, Booth JR. Deficient orthographic and phonological representations in children with dyslexia revealed by brain activation patterns. Journal of Child Psychology and Psychiatry and Allied Disciplines. 2006; 47:1041–1050.
5. Catani M, Jones, D K DK, ffytche DH. Perisylvian language networks of the human brain. Annals of Neurology. 2005; 57:8–16. [PubMed: 15597383]
6. Deutsch DK, Dougherty RF, Bammer R, Siok WT, Gabrieli JD, Wandell B. Children's reading performance is correlated with white matter structure measured by diffusion tensor imaging. Cortex. 2005; 41:354–363. [PubMed: 15871600]
7. Fingelkurts A, Fingelkurts A, Krause C, Kaplan A, Borisov S, Sama M. Structural (operational) synchrony of alpha EEG activity during an auditory memory task. Neuroimage. 2003; 20:529–542. [PubMed: 14527613]
8. Horwitz B, Rumsey JM, Donohue BC. Functional connectivity of the angular gyrus in normal reading and dyslexia. Proceeding of the National Academy of Sciences. 1998; 95:8939–8944.
9. Lachaux JP, Rodriguez E, Martinerie J, Varela FJ. Measuring phase synchrony in brain signals. Hum Brain Mapp. 1999; 8:194–208. [PubMed: 10619414]
10. Latora V, Marchiori M. Efficient behavior of small-world networks. Phys Rev Lett. 2001; 39:62–79.
11. Lawes IN, Barrick TR, Murugam V, Spierings N, Evans DR, Song M, Clark CA. Atlas-based segmentation of white matter tracts of the human brain using diffusion tensor tractography and comparison with classical dissection. Neuroimage. 2008; 39:62–79. [PubMed: 17919935]
12. Le Van Quyen M, Foucher J, Lachaux J, Rodriguez E, Lutz A, Martinerie J, Varela FJ. Comparison of Hilbert transform and wavelet methods for the analysis of neuronal synchrony. J Neurosci Methods. 2001; 111:83–98. [PubMed: 11595276]
13. Micheloyannis S, Pachou E, Stam CJ, Vourkas M, Erimaki S, Tsirka V. Using graph theoretical analysis of multi channel EEG to evaluate the neural efficiency hypothesis. Neurosci Lett. 2006; 402:273–277. [PubMed: 16678344]
14. Newman MEJ. Fast algorithm for detecting community structure in networks. Phys Rev. E. 2004; 69:066133.
15. Niogi SN, McCandliss BD. Left laterized white matter microstructure accounts for individual differences in reading ability and disability. Neuropsychologia. 2006; 44:2178–2188. [PubMed: 16524602]
16. Pugh KR, Mencl WE, Shaywitz BA, et al. The angular gyrus in developmental dyslexia: task-specific differences in functional connectivity within posterior cortex. Psychological Science. 2000; 11:51–56. [PubMed: 11228843]
17. Shaywitz BA, Shaywitz SE, Pugh KR, Mencl WE, Fulbright RK, Skudlarski P, Constable RT, Marchione KE, Fletschr JM, Lyon GR, Gore JC. Disruption of posterior brain systems for reading in children with developmental dyslexia. Biological Psychiatry. 2002; 25:101–110. [PubMed: 12114001]
18. Schoffelen J-M, Gross J. Source connectivity analysis with MEG and EEG. Human Brain Mapp. 2009; 30:1857–1865.
19. Simos PG, Fletcher JM, Bergman E, Breier JI, Foorman BR, Castillo EM, Davis RN, Fitzgerald M, Papanicolaou AC. Dyslexia-specific brain activation profile become normal following successful remedial training. Neurology. 2002; 58:1203–1213. [PubMed: 11971088]
20. Simos PG, Fletcher JM, Sarkari S, Billingsley RL, Denton CA, Papanicolaou AC. Altering the brain circuits for reading through intervention: a magnetic source imaging study. Neuropsychology. 2007a; 21:485–496. [PubMed: 17605581]

21. Simos PG, Papanicolaou AC, Fletcher JM, Sarkari S, Denton C. Intensive instruction affects brain magnetic activity associated with reading fluency in children with dyslexia. Journal of Learning Disabilities. 2007b; 40:37–48. [PubMed: 17274546]

22. Sporns O, Zwi JD. The small world of the cerebral cortex. Neuroinformatics. 2004; 2:145–162. [PubMed: 15319512]

23. Stam CJ, Nolte G, Daffertshofer A. Phase lag index: assessment of functional connectivity from multi channel EEG and MEG with diminished bias from common sources. Hum Brain Mapp. 2007a; 28:1178–1193. [PubMed: 17266107]

24. Stam CJ, Reijneveld JC. Graph theoretical analysis of complex networks in the brain. Nonlinear Biomed Phys. 2007b; 1:3. [PubMed: 17908336]

25. Steinbrink C, Vogt K, Kastrup A, Müller HP, Juengling FD, Kassubek J, Riecker A. The contribution of white and gray matter differences to developmental dyslexia: insights from DTI and VBM at 3.0 T. Neuropsychology. 2008; 46:3170–3178.

26. Strogatz SH. Exploring complex networks. Nature. 2001; 410:268–276. [PubMed: 11258382]

27. Wechsler, D. Wechsler Abbreviated Scale of Intelligence (WASI). San Antonio, TX: The Psychological Corporation; 1999.

28. Woodcock, RW.; McCrew, KS.; Mather, N. Psychoeducational tests of Achievement – III. Itasca, IL: Riverside; 2000.

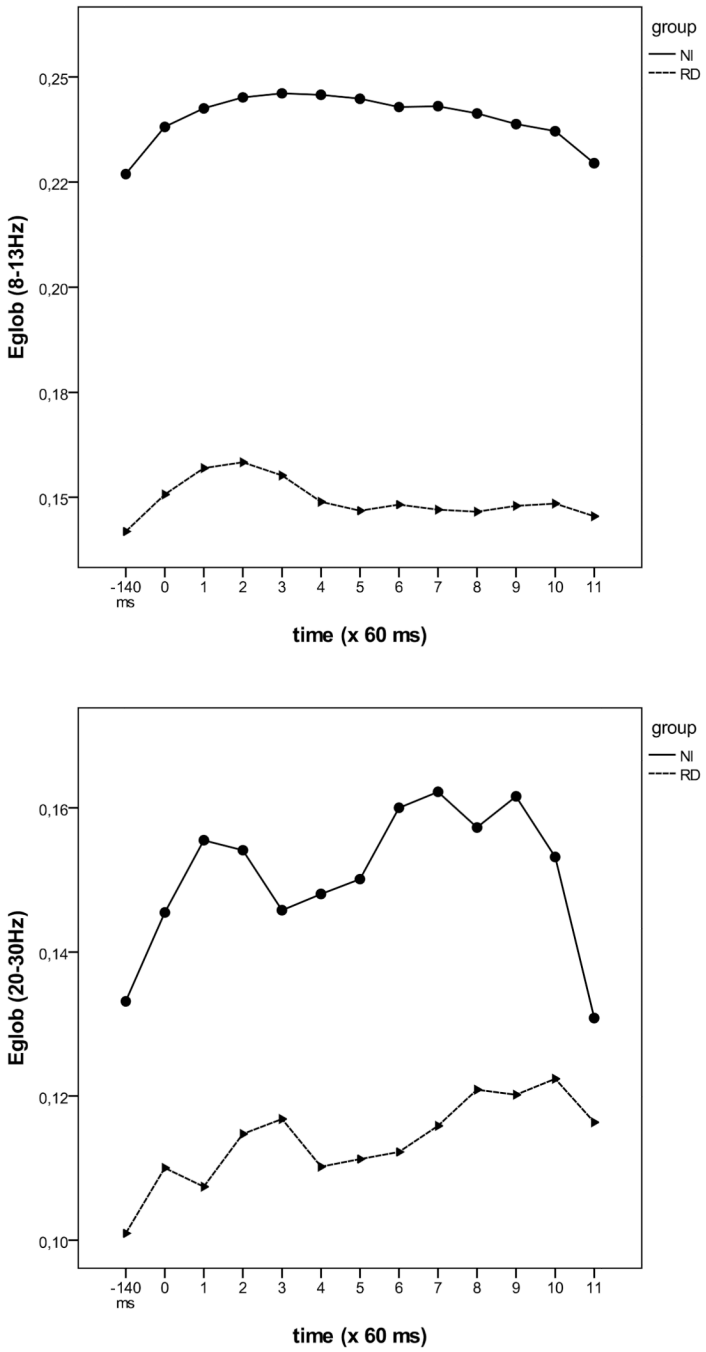

Figure 1.

Time course of mean raw (non-normalized) Global Efficiency (E_{glob}) estimates computed from single-epoch MEG recordings in the alpha (upper panel) and gamma bands (lower panel) indicating higher values for typical (NI) than students with severe reading difficulties (RD). Similar time courses were noted for Local Efficiency (E_{loc}, alpha and gamma bands) and Mean Degree (K, alpha band only) values across groups.

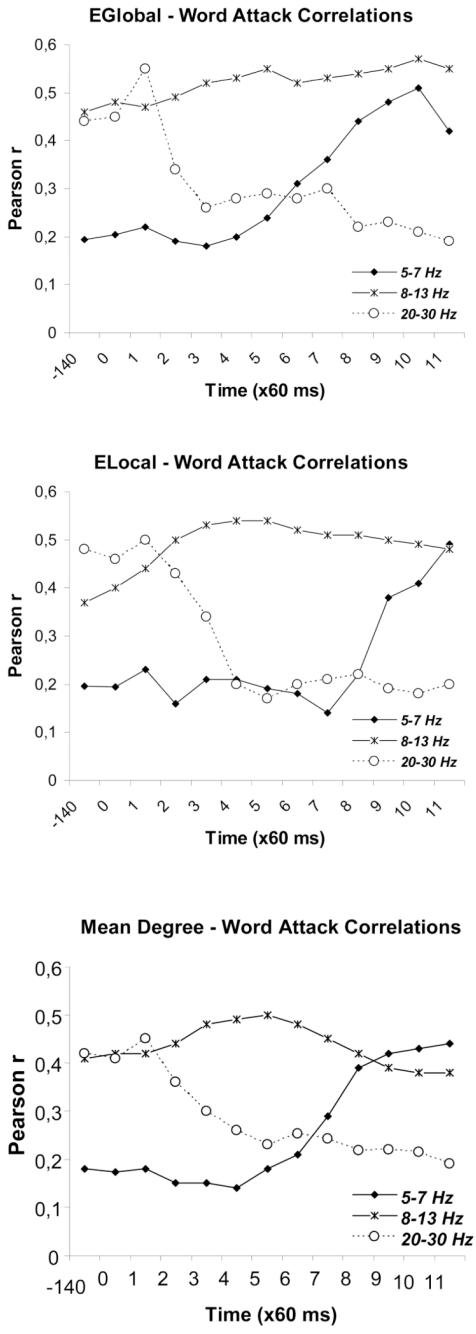

Figure 2.

Time course of correlations between WJ-III Word Attack scores and graph metrics (Global Efficiency [E_{Global}], Local Efficiency [E_{Local}], and mean degree [K]) for the entire sample of participants. Values computed for signals in the theta band are indicated by filled diamonds, in the alpha band by asterisks, and in the beta band by open circles. The first time point corresponds to the prestimulus baseline (−140 to 0 ms).

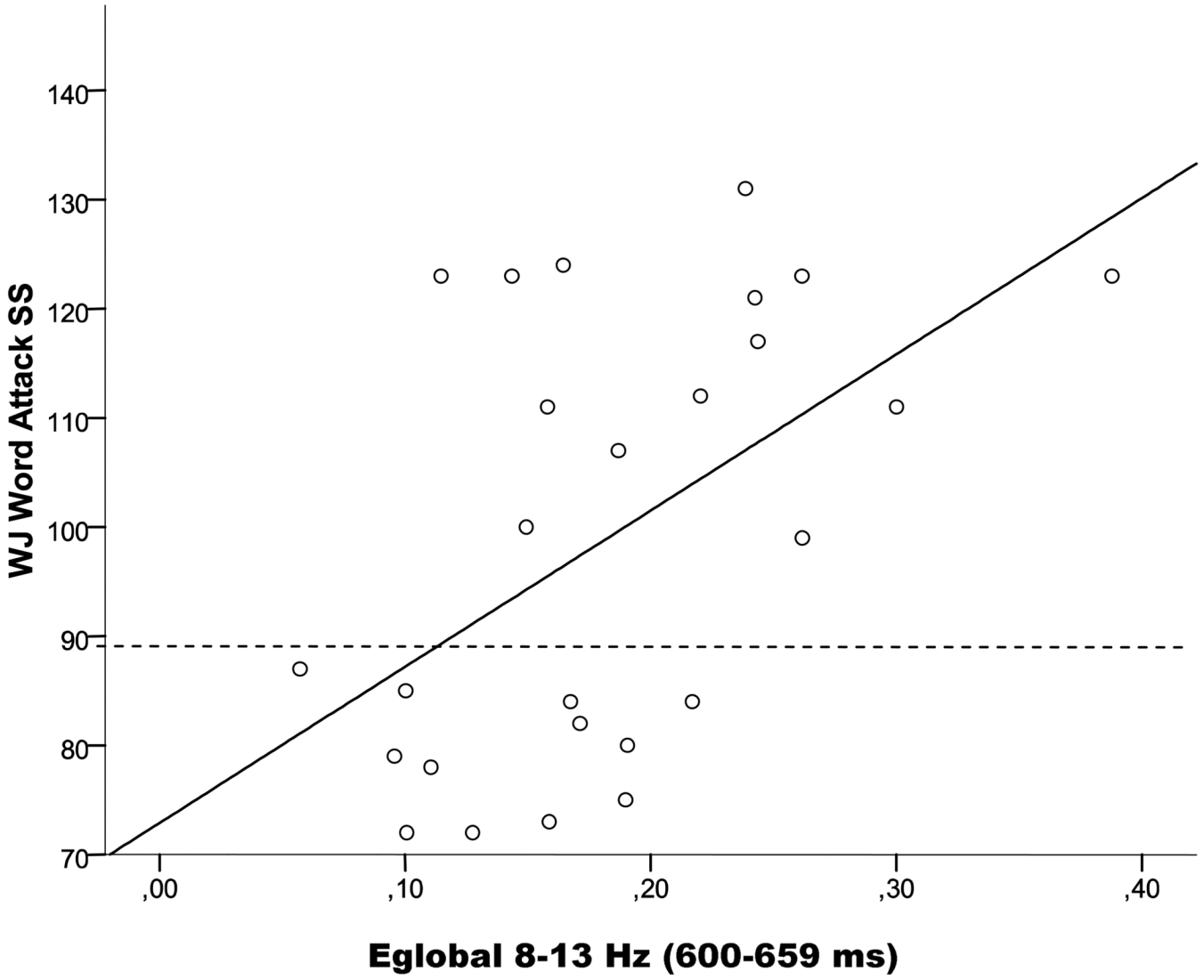

Figure 3.
Scatter plot of single-subject data illustrating the regression of WJ-III Word Attack scores over Global Efficiency indices estimated in the alpha band during late stages of stimulus processing (600–659 ms after stimulus onset) from single-epoch data during pseudoword reading. The dotted line separates typical and reading impaired readers.

Table 1

Demographic and psychoeducational data for typical (NI) and reading disabled students (RD).

	Group	Mean	SD
Age (mo)	NI	117.08	29.3
	RD	127.22	25.7
LWID**	NI	109.46	10.0
	RD	67.89	17.3
WA**	NI	116.46	9.9
	RD	79.89	4.4
Composite**	NI	112.96	8.7
	RD	73.94	10.4
VIQ	NI	109.15	13.9
	RD	101.56	13.6
PIQ	NI	102.85	9.0
	RD	99.11	11.7
% Correct Letter Sound	NI	93.44	11.7
	RD	92.56	15.7
% Correct Pseudowords**	NI	87.61	11.1
	RD	43.55	6.6

Group differences:

** $p < .001$.

Abbreviations, LWID: Woodcock-Johnson Letter-Word Identification, WA: Woodcock-Johnson Word Attack, Composite: Woodcock-Johnson Basic Reading composite.